CONDUCTION IN COMPOSITES WITH HIGHLY CONDUCTIVE SHORT FIBRES: COMPARISON BETWEEN EXPERIMENTS, DISCRETE ELEMENT SIMULATION AND ANALYTICAL SOLUTION

Jean-Pierre Vassal[1], Laurent Orgéas[1], Pierre Dumont[2], Denis Favier[1], Véronique Michaud[3]

[1]Laboratoire Sols-Solides-Structures-Risques (3SR), CNRS – Université de Grenoble (INPG – UJF)
BP 53, 38041 Grenoble cedex 9, France
[2]Laboratoire de Génie des Procédés Papetiers (LGP2), CNRS – INPG – EFPG
BP 65, 461, rue de la Papeterie, 38402 Saint-Martin-d'Hères cedex, France
[3]Laboratoire de Technologie des Composites et Polymères (LTC) – Ecole Polytechnique Fédérale de Lausanne (EPFL), CH-1015 Lausanne, Switzerland

ABSTRACT

Heat transfer properties of polymer composites reinforced with highly conductive short fibres are studied in this work. For that purpose, thin plates made up of a high concentration of copper fibres immerged in a PMMA matrix are processed with controlled fibrous microstructures. The thermal heat transfer properties of these plates through their midplane are studied both with a specially designed testing apparatus and an inverse modelling technique. Experimental results underline the influences of the fibre aspect ratio, content and orientation on the effective conductivity tensor of the as-processed composites. They are compared with predictions given by an analytical conductivity model, deduced from an upscaling technique and discrete element simulations.

1. INTRODUCTION

Increasing thermal or electrical conductivity of polymer composites by using a high content (*i.e.* largely above the percolation threshold) of highly conductive particles such as short carbon fibres, carbon nanotubes or short metallic fibres can be a potentially very interesting technological solution to replace metallic parts. However, an important limitation in the development of these composites is ascribed to the difficulty to accurately predict their effective conductivity.

- The first reason is that analytical conductivity models are missing. Indeed, if numerous analytical models have been proposed to estimate thermal conductivity in dilute suspensions or near the percolation threshold, they are generally not adapted to the high volume fraction of fibres of industrial materials. To the best of our knowledge, the unique analytical model dedicated to highly concentrated composites with highly conductive fibres has been proposed in [1]. However, this model is restricted to 2D microstructures and some of its fitting parameters are difficult to get from the microstructure. More recently, by extending concepts initially introduced for granular materials [2], 3D analytical conductivity models for highly concentrated fibrous media with fibre-fibre interfacial barriers have been proposed from an upscaling process [3] and from discrete element simulations [4-5]. However, these models have not been compared to reliable experimental data yet.
- Model predictions are usually compared with experimental data coming from samples that have been produced under industrial processing conditions, e.g. injection moulding. Firstly, induced fibrous microstructures are difficult to observe and quantify due to the opacity of polymers that are generally used.

Secondly, they are also very difficult to control and may exhibit very strong heterogeneities [6] which can induce high experimental scattering.

In order to circumvent the above experimental difficulties, we have processed a model composite made up of a PMMA matrix reinforced with short copper fibres. The transparent matrix allows direct observation of fibrous microstructures. The processing route allows to produce samples with homogeneous various fibre contents, aspect ratios and orientations (section 2). Samples were then subjected to transient unidirectional thermal loading with a specially designed testing apparatus and an inverse modelling technique was used in order to estimate their effective in-plane conductivity from experiments (section 3). Results are given in section 4. Experimental trends are then compared with the prediction of an analytical model developed in [4-5]. This model was deduced from discrete element simulation performed on Representative Elementary Volumes (REV's) of the considered fibrous microstructures.

2. MATERIALS: PROCESSING ROUTE AND CHARACTERISATION

In order to characterise easily fibrous microstructures, composites with a transparent polymer matrix were processed. A thermoplastic PMMA (Altuglas, Atofina) was chosen because of its excellent transparency. This matrix was reinforced with short and straight copper fibres having circular cross sections. Copper fibres exhibit a very high thermal conductivity compared to the one of the PMMA polymer (see table 1). The fibre diameter d equals 0.25 mm and two fibre lengths l have been studied, i.e. l = 10 mm and l = 20 mm.

Constituent	Density [kg m^{-3}]	Thermal conductivity [W m^{-1} K^{-1}]	Specific Heat [J kg^{-1} K^{-1}]
PMMA	1190	0.19	1450
Copper fibres	8960	400	385

Table 1 – Physical properties of constituents

To obtain samples displaying homogeneously distributed fibres and controlled fibre volume fraction and orientation, a special processing route extensively described in [7] was adopted. Resulting cylindrical plates (diameter of 120 mm, thickness of 3.5 mm) exhibit no visible pores and nearly 2D planar fibrous microstructures, *i.e.* all fibres' centrelines can be considered as almost parallel to the midplane of the plates ($\mathbf{e}_1$, $\mathbf{e}_2$). In order to avoid boundary effects, square samples (66×66×3.5 mm^3) have been cut inside the cylinders. Their edges were parallel with the principal axes of the fibre orientation. As an example, figure 1 gives two produced samples with a volume fraction of fibres f = 0.1 and a fibre aspect ratio l/d = 40, exhibiting 2D planar random (figure 1(a-b)) and oriented (figure 1(d-e)) fibre orientations. Photographs displayed in this figure show that the fibrous microstructures are very easy to observe. One can also notice the very good in-plane (figure 1(a,d)) and through-the-thickness (figure 2) homogeneities of samples. Lastly, figure 1 shows that the processing route does not induce significant bending of fibres, which can be considered as straight.

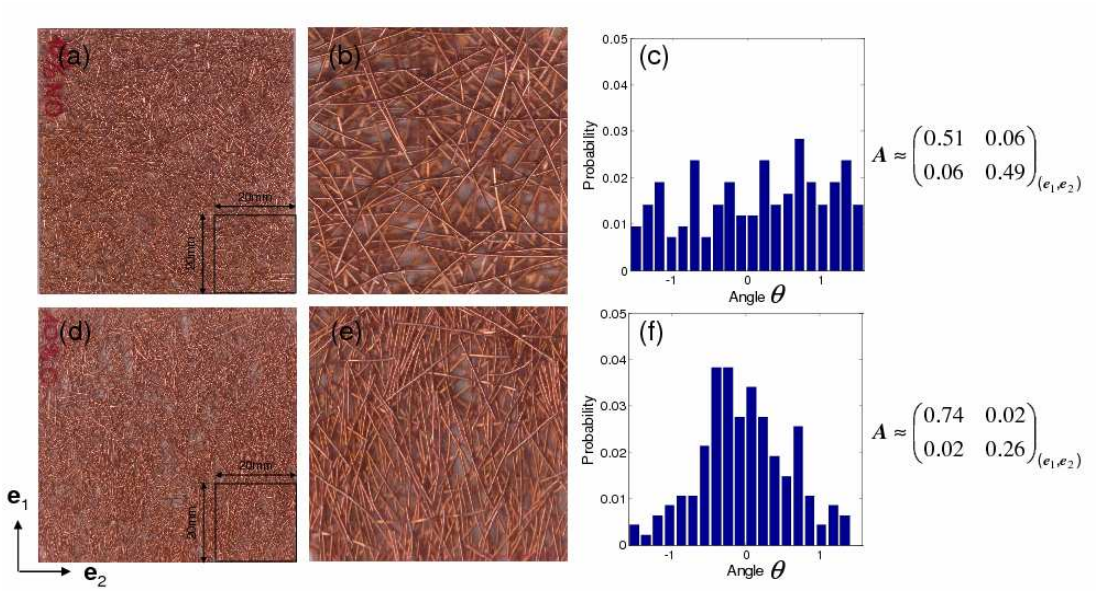

Figure 1 – Examples of samples ($f \approx 0.1$). In-plane homogeneity of samples is presented in (a) and (d) and zooms of the black lines boxes are presented in (b) and (e) respectively for isotropic and oriented samples. Corresponding orientation distribution functions as well as second order orientation tensors **A** are given in (c) and (f) respectively.

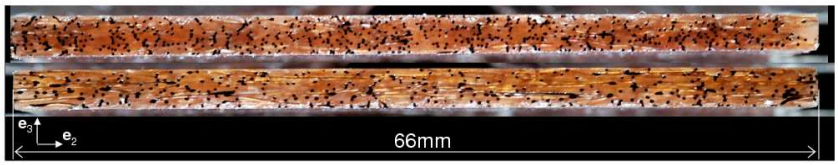

Figure 2 – Examples of samples cut in the ($\mathbf{e}_2$, $\mathbf{e}_3$) plane, showing their homogeneity through their thickness homogeneity of samples. Top: oriented sample with $f \approx 0.15$, bottom: isotropic sample with $f \approx 0.10$.

Samples with various volume fraction of fibres f ranging from 0.02 to 0.23 were processed. Due to the very high density contrast between the fibres and the matrix, the fibre content f was easily obtained from the measurements of volumes and weights of the samples (volumes are measured by weighting the samples while they are immersed in water).

As illustrated in figure 1, two types of fibre orientation were studied. The 2D orientation of fibres was characterised using scanned pictures of samples and the software ImageJ. As presented in [7], the 2D orientation vectors $\mathbf{p}_i = \cos\theta_i\, \mathbf{e}_1 + \sin\theta_i\, \mathbf{e}_2$ of N =120 fibres were detected by manual picking for each sample. Therewith, it was possible to obtain discrete histograms of the 2D Fibre Orientation Distribution (FOD) and discrete expression of the 2D second order fibre orientation tensor **A** [7-8]:

$$\mathbf{A} = \frac{1}{N}\sum_{N} \mathbf{p}_i \otimes \mathbf{p}_i \,. \qquad (1)$$

As an example, we have reported in figure 1(c) and 1(f) the FODF and the orientation tensors corresponding to the 2D planar random and the oriented fibrous microstructures shown in figure 1(a) and 1(d), respectively. In the following, only the second order orientation tensor will be used. The average orientation tensor obtained for planar-isotropic $\mathbf{A}^{iso}$ and aligned $\mathbf{A}^{ali}$ samples are respectively:

$$\mathbf{A}^{iso} = \begin{bmatrix} 0.49^{\pm 0.04} & 0^{\pm 0.02} \\ 0^{\pm 0.02} & 0.51^{\pm 0.04} \end{bmatrix}_{\mathbf{e}_1,\mathbf{e}_2} \quad \text{and} \quad \mathbf{A}^{ali} = \begin{bmatrix} 0.70^{\pm 0.04} & 0^{\pm 0.02} \\ 0^{\pm 0.02} & 0.30^{\pm 0.04} \end{bmatrix}_{\mathbf{e}_1,\mathbf{e}_2} \tag{2}$$

3. ESTIMATION OF THE IN-PLANE THERMAL CONDUCTIVITY

The in-plane effective conductivity tensors of the produced samples were determined following the experimental method proposed in [9]. The method consists in four steps:

1. A one-dimensional transient heat flow is imposed to the sample. This was achieved with a specially designed testing apparatus, which oversimplified scheme is given in figure 3(a). Such an experimental setup ensures that edge effects and lateral heat losses are negligible. Edge effects are reduced by using sufficiently large samples with respect to the length of portions of fibres between two consecutive fibre-fibre contacts [5]. Heat losses are reduced (i) by making experiments in vacuum so that convection is limited and (ii) by adding a reflecting layer (thin metallic sheet) on the insulating walls of the apparatus so that radiation losses are limited (see figure 3(a)). At initial state, the whole setup and the tested sample are at the same constant temperature, *i.e.* 20°C. Then, the faces normal to the heat flow direction are subjected to a sudden thermal difference of 30°C using thermally regulated fluids at $T_0 = 20$°C and $T_1 = 50$°C (see figure 2(a)).
2. The time evolution of the temperature of the sample is recorded at different positions located at constant positions along the heat flow direction. This was achieved with 4 thermocouples (see figure 2(a), $\Delta h = 10$ mm). A typical time evolution of the temperature given by the thermocouples is shown in figure 2(b) for an aligned sample ($l/d = 40$ and $f = 0.16$) tested in the main direction of fibres.
3. An inverse numerical approach is used to estimate the thermal conductivity Λ^e in the flow direction. For that purpose, a 1D Finite Element model of the experiment was built with the commercial FE code Comsol and the standard heat balance equation
$$C^e \frac{\partial T}{\partial t} = \Lambda^e \frac{\partial^2 T}{\partial x^2} \tag{3}$$
was solved along the length of the tested sample, experimental data recorded by the two external (*i.e.* the most distant) thermocouples being used as time-evolving boundary conditions. To run the simulations, the effective volumetric heat capacity C^e of the sample was estimated by a simple volume averaging [3]. An optimisation algorithm implemented in Matlab was used to compute the effective conductivity Λ^e that minimises the error between experimental and numerical temperatures of the two central thermocouples. As an example, we report in figure 3(b) the best fit of experimental data obtained by this optimisation procedure (grey lines). As shown from this figure, the fit is fairly good. By doubling the measurements, the relative error on the estimated thermal conductivity was found to be ±10%.
4. The measure was repeated in the two in-plane principal directions of fibre orientation ($\mathbf{e}_1$ and $\mathbf{e}_2$) in order to obtain the in-plane components Λ_1^e and Λ_2^e of the thermal conductivity tensor.

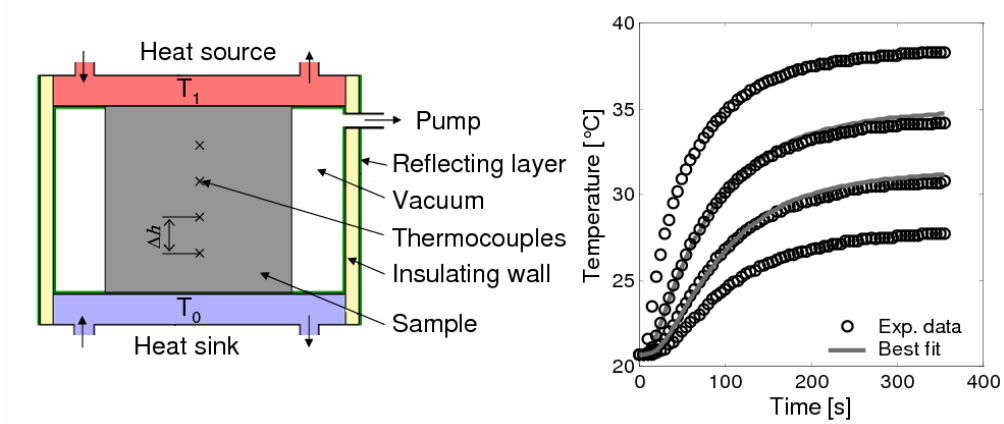

Figure 3 – Scheme of the experimental device used to estimate the thermal conductivity (left). Example of experimental data that have been obtained for a composite with f = 10%, planar random orientation (right). The grey lines plotted in this graph are the best fits obtained with the inverse method.

4. RESULTS

Experimental in plane conductivities Λ_1^e and Λ_2^e for 2D planar random and 2D aligned samples (orientation tensors being respectively given by (2a) and (2b)) are plotted in figure 4 (symbols) for fibres displaying aspect ratios l/d = 40 (figure 4(a)) and l/d = 80 (figure 4(b)).

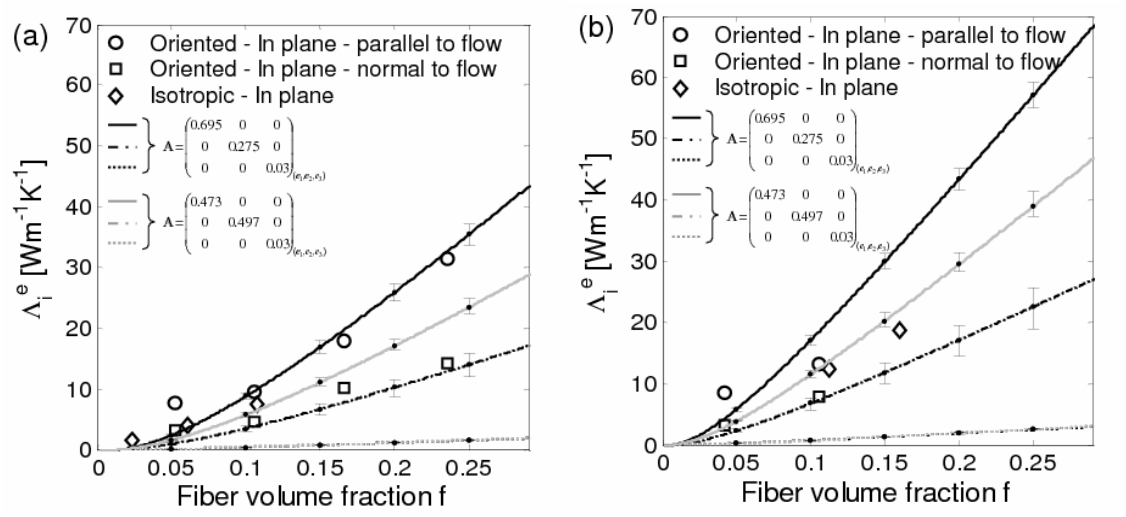

Figure 4 – Evolution of the effective thermal conductivity with the volume fraction of fibres for different orientations and for aspect ratios l/d = 40 (a) and 80 (b): planar-isotropic (grey lines, diamond symbols) and planar-aligned (black lines, circle and square symbols) microstructures. Lines represent the predictions given by the analytical model (4-8) with a constant heat transfer coefficient h =1.65 10^4 W m^{-2} K^{-1}. Dotted and dashed-dotted lines represent the predicted through-the-thickness effective conductivity.

These results bring up the following comments.

- Rather high thermal conductivities can be obtained, even at low fibre contents. For example a thermal conductivity of almost 10 Wm^{-1}K^{-1} is obtained for l/d = 80 and f = 0.04 in case of oriented samples.

- Whatever the orientation **A** and aspect ratio of fibres l/d are, and for fibre volume fraction f higher than 0.05, increasing the fibre content causes a nearly linear increase of the conductivity.
- Whatever the fibre content f and aspect ratio l/d are, the in-plane thermal conductivity tensor exhibits strong anisotropy when fibrous microstructures are oriented ($\Lambda_1^e > \Lambda_2^e$) whereas it displays 2D isotropy when the sample has a 2D planar random fibre orientation ($\Lambda_1^e = \Lambda_2^e$). Likewise, conductivities of the 2D planar random samples always lie between major and minor conductivities of oriented samples.
- Whatever the volume fraction and orientation of fibres are, increasing the fibre aspect ratio l/d increase the thermal conductivity. For example, planar isotropic sample with $f = 0.11$ and $l/d = 80$ (figure 4(b)) has an in-plane conductivity which is 20% higher than that of samples having the same orientation, fibre content and an aspect ratio $l/d = 40$ (figure 4(a)).

5. COMPARISON WITH AN ANALYTICAL MODEL

Experimental results obtained in this study are now compared to the analytical hybrid model we have proposed recently [5]. This semi-empirical conductivity model is dedicated to conduction in concentrated fibrous materials with highly conductive short, straight and slender fibres (of thermal conductivity λ). It can account for possible fibre-fibre contact resistances. In this model, the bulk conductivity of the matrix is neglected, and the complex heat transfers occurring in the neighbouring of fibre-fibre contacts are modelled by a heat transfer coefficient h. This model was established from a rigorous upscaling process [3] and from discrete element simulations performed on representative fibrous microstructures [4-5]. It assumes that fibres are homogeneously distributed and that their corresponding FOD follow Gaussian distributions. Thus, whatever the quality of heat transfers at fibre-fibre contacts, the effective conductivity tensor reads:

$$\mathbf{\Lambda}^e = \frac{1}{2}\left(\frac{1}{1+10\overline{\overline{C}}_\alpha fB}\mathbf{\Lambda}^{eIII} + \frac{1}{1+\dfrac{1}{10\overline{\overline{C}}_\alpha fB}}\mathbf{\Lambda}^{eI} \right) \tag{4}$$

where the Biot number B is defined as

$$B = \frac{4hl}{\lambda\pi\langle\sin\theta\rangle\overline{\overline{C}}_\alpha} \tag{5}$$

and where the effective conductivity tensors

$$\mathbf{\Lambda}^{eI} = f\lambda\left(1-\frac{1}{\overline{\overline{C}}_\alpha}\right)\mathbf{A} \quad \text{and} \quad \mathbf{\Lambda}^{eIII} = C_1\frac{d^2}{\langle\sin\theta\rangle}h\frac{l^2}{6}\left(1-\frac{1}{\overline{\overline{C}}_\alpha}\right)\mathbf{A} \tag{6}$$

stand for the effective conductivity when fibre-fibre contacts are perfect or very poor, respectively. These analytical expressions were obtained by assuming affine distribution of the temperature field [4]. The microstructure descriptors $\langle\sin\theta\rangle$, $\overline{\overline{C}}_\alpha$ and

C_1 involved in the above equations represent respectively the average value of the sine of the angles between contacting fibres, the average number of fibre-fibre contacts per fibre, and the number of fibre-fibre contacts per unit of volume. $\overline{C}_\alpha$ and C_1 can be estimated using the statistical tube model [10-12]:

$$\overline{C}_\alpha = 4f\left(\frac{2l}{\pi d}\phi_1 + \phi_2 + 1\right) \quad \text{and} \quad C_1 = \frac{f}{\pi d l}\overline{C}_\alpha \tag{7}$$

It was shown that the microstructure descriptors $\langle \sin\theta \rangle$, ϕ_1 and ϕ_2 could be expressed as functions of the two minor principal values A_I and A_{II} of the 3D fibre orientation tensor, for wide ranges of fibre concentrations, aspect ratios and orientations [5]:

$$\begin{aligned}
\phi_1 &= (-6.12A_{II}^2 + 4.49A_{II} - 2.49)A_I^2 \\
&+ (4.46A_{II}^2 - 4.87A_{II} - 2.23)A_I \\
&- 2.47A_{II}^2 + 2.22A_{II} + 0.14 \\
\phi_2 &= (-5.2A_{II}^2 + 3.58A_{II} - 1.07)A_I^2 \\
&+ (3.55A_{II}^2 - 0.79A_{II} - 1.26)A_I \\
&+ 1.09A_{II}^2 - 1.27A_{II} + 1.00 \\
\langle \sin\theta \rangle &= (-6.85A_{II}^2 + 5.23A_{II} - 2.78)A_I^2 \\
&+ (5.10A_{II}^2 - 5.50A_{II} - 2.45)A_I \\
&- 2.76A_{II}^2 + 2.44A_{II} + 0.08
\end{aligned} \tag{7}$$

Thus, in this model, the only fitting parameter is *h*, *i.e.* the heat transfer coefficient which reflects heat transfers in fibre-fibre contact zones. If $h \to \infty$, contacts between fibres are perfect and if $h \to 0$, contacts are perfectly insulating. In this work, we fixed *h* to a constant value, whatever the fibre content, orientation and aspect ratio, for the sake of simplicity. Its value was determined in order to obtain the best fit of experimental results: $h = 1.65\ 10^4$ W m^{-2} K^{-1}. Predictions given by the model (4-8) have been plotted in figure 4. We have assumed here that fibrous networks have a planar fibre orientation so that the principal component of the 3D fibre orientation tensor along the thickness of the plates is arbitrarily set to a weak value of 0.03 [13]. Error bars represent calculations made for the extreme values of the measured 2D orientation tensors (2). As shown from this figure, the analytic model shows a rather good capability in reproducing experimental data at high fibre concentrations $f \geq 0.05$. It is able to capture the influence of both the orientation, the aspect ratio and the volume fraction of fibres. Expected conductivities in direction normal to plane (transverse conductivity) were also calculated and plotted in figure 4 (dotted and dashed-dotted lines). This latter result shows that transverse conductivity is much smaller and seems to be less sensitive to in-plane orientation of fibres.

6. CONCLUSION

In this contribution, model composites made up of highly conductive slender copper fibres impregnated by a poorly conductive and transparent PMMA matrix was produced. Their thermal in-plane conductivities were characterized using a special testing apparatus. In-plane microstructure anisotropy was shown to be closely linked to

thermal conductivity anisotropy. Moreover the experiments underlined the leading role of fibre volume fraction and the second order role of fibre aspect ratio on thermal conductivity. The predictions from an analytical semi-empirical model which takes into account the orientation, aspect ratio, and volume fraction of fibres as well as fibre-fibre thermal resistances, were compared to experiments. Using only one fitting parameter, this model can reproduce experiments well.

ACKNOWLEDGEMENTS

Jean-Pierre Vassal would like to thank the Région Rhône-Alpes (France) for its support of this work through the research grant it provided. The authors also gratefully acknowledge the European Research Group "HetMat" for its financial support.

REFERENCES

1. M. Weber and M.S. Kamal, "Estimation of the volume resistivity of electrically conductive composites" *Polym. Compos.*, Vol. 18, pp 711-725, 1997.
2. G.K. Batchelor, F.R.S. O'Brien, and R.W. O'Brien, "Thermal or electrical conduction through a granular material, *Proc. R. Soc. Lond. A.*, Vol. 15, pp 355-313, 1977.
3. J.-P. Vassal, L. Orgéas, D. Favier, J.-L. Auriault and S. Le Corre, "Upscaling the diffusion equations in particulate media made of highly conductive particles. I: theoretical aspects" *Phys. Rev. E*, 2008;77:011302.
4. J.-P. Vassal, L. Orgéas, D. Favier, J.-L. Auriault and S. Le Corre, "Upscaling the diffusion equations in particulate media made of highly conductive particles. II: application to fibrous materials" *Phys. Rev. E*, 2008;77:011303.
5. J.-P. Vassal, L. Orgéas, and D. Favier, "Modelling microstructure effects on the conduction in fibrous materials with fibre-fibre interfacial barriers" *Modelling Simul. Mater. Sci. Eng.*, 2008;16:035007.
6. F. Danes, B. Garnier, T. Dupuis, P. Lerendu, and T.-P. Nguyen, "Non-uniformity of the filler concentration and of the transverse thermal and electrical conductivities of filled polymer plates" *Compos. Sci. Technol.*, 2005;65:945-51.
7. P. Dumont, J.-P. Vassal, L. Orgéas, V. Michaud, D. Favier, and J.A.-E. Manson, "Processing, characterization and rheology of transparent concentrated fibre bundle suspensions" *Rheol. Acta*, 2007; 46: 639-41.
8. S.G. Advani and C.L. Tucker "The use of tensors to describe and predict fiber orientation in short fiber composites" *J. Rheol.*,1987;3:751–84.
9. R.D. Sweeting and X.L. Liu "Measurement of thermal conductivity for fibre-reinforced composites" *Compos. Part A*, 2004; 35:933–38.
10. M. Doi and S.F. Edwards "Dynamics of rod-like macromolecules in concentrated solution" *J. Chem. Soc. Faraday Trans. II*, 1978;74:560–70.
11. S. Ranganathan and S. G. Advani "Fiber-fiber interactions in homogeneous flows of non-dilute suspensions" *J. Rheol.* 1991;35:1499–22.
12. S. Toll "Note: On the tube model for fiber suspensions" *J. Rheol.*, 1993; 37:123–25.
13. S.G. Advani "*Flow and Rheology in Polymer Composites Manufacturing*", volume 10 of Composite Materials Series. Elsevier, 1994.